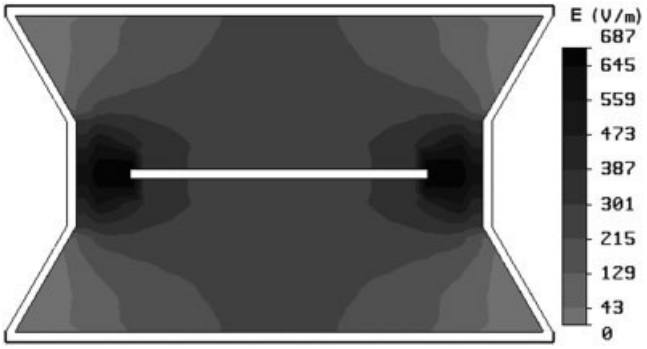

Figure 6 The electric field distribution of the TEM mode

Comparing the results in Table 1 it can be seen that satisfactory results are obtained by the CMM presented in this paper.

When the outer conductors are the same size and characteristic impedances are both 50 Ω, the comparison of cutoff frequency between novel and conventional TEM cell are presented in Table 2. Here, L equals 10 cm and I equals 2 cm.

When $L = 10$ cm, $H = 6$ cm, $I = 2$ cm, $\theta = 60°$, and the input power is 1 W, the electric field distribution of TEM mode in the novel TEM cell is shown in Figure 6. According to the definition of uniform field in IEC 61000-4-20, the uniform area in Figure 6 is 4.55 cm $\times$2.9 cm. In the conventional TEM cell which has the same cutoff frequency and length–width ratio, the uniform area is 5.10 cm $\times$ 2.46 cm, smaller than that of the novel one.

5. CONCLUSION

In order to study the kinetics of microwave chemistry, new devices with a higher cutoff frequency and a larger area of uniform electromagnetic field are needed. In this paper, we propose a novel TEM cell to satisfy these conditions and used an analytical method based on a three-step conformal mapping to calculate the characteristic impedance of the TEM cell. Two methods were used to validate the analytical solution. First, the FEM numerical method was used to calculate the characteristic impedance. The comparison between the analytical and numerical calculation showed the analytic solution gave very precise results. Then, when the configuration of the TEM cell degenerated to a conventional TEM cell, the calculation of characteristic impedance agreed very well with the results previously published in the literatures. Further work, such as the calculation of the field distribution in a test tube and the design of taper connected with the coaxial line will be shown in the future.

ACKNOWLEDGMENT

This project was supported by National Science Foundation of China under Grants 60125102 and 60471045.

REFERENCES

1. X.-Q. Yang and K.-M. Huang, Study on the key problems of interaction between microwave and chemical reaction, Chin Jof Radio Sci 21 (2006), 802-809.
2. Q.-H. Jin, S.-S Dai, and K.-M. Huang, Microwave chemistry, Science Press, Beijing, 1999.
3. Z.-B. Zhang, L.-X. Zhou, Y.-R. Li, C.-H. Yan, and M. Zhang, The synthesis of diphenyl thiourea under irradiation of different frequency microwave, J Yangzhou Univ (Natural Science Edition), 3 (2000), 14-16.
4. X.-D. Cai and J.-Y. Li, Analysis of asymmetric TEM cell and its optimum design of electric field distribution, IEE Proc 136 (1989), 191-194.
5. E. Costamagna and A. Fanni, Asymmetric TEM cell impedance calculation, IEE Proc 137 (1990), 318-320.
6. S.K. Das and B.N. Das, Analysis of the effects of septum thickness on impedance and fields of TEM mode inside an asymmetric TEM cell, IEE Proc-H 140 (1993), 347-353.

INTERNAL SHORTED PLANAR MONOPOLE ANTENNA EMBEDDED WITH A RESONANT SPIRAL SLOT FOR PENTA-BAND MOBILE PHONE APPLICATION

Chih-Hsien Wu and Kin-Lu Wong
Department of Electrical Engineering, National Sun Yat-Sen University, Kaohsiung 804, Taiwan, Republic of China; Corresponding author: wuch@ema.ee.nsysu.edu.tw

Received 20 July 2007

ABSTRACT: *An internal shorted planar monopole antenna embedded with a resonant spiral slot for GSM850/900/DCS/PCS/UMTS operation in the mobile phone is presented. The planar monopole is printed on an FR4 substrate of small size 10 $\times$ 45 mm^2, and a spiral slot of length 108 mm is embedded therein. The planar monopole is then placed above and perpendicular to the top edge, with a small distance of 7 mm, of the system ground plane of the mobile phone to operate as an internal antenna. A coupled feed printed on the top no-ground portion of the system circuit board is used to excite both the planar monopole and the spiral slot to generate two wide bands covering GSM850/900 and DCS/PCS/UMTS operation, respectively. The antenna is also suitable to integrate with the associated electronic components, such as the speaker, to achieve a compact integration of the antenna inside the mobile phone. Experimental and SPEAG SEMCAD-X simulation results of the proposed antenna are presented. The user's hand effects on impedance and radiation characteristics of the antenna are also analyzed.* © 2007 Wiley Periodicals, Inc. Microwave Opt Technol Lett 50: 529–536, 2008; Published online in Wiley InterScience (www.interscience.wiley.com). DOI 10.1002/mop.23126

Key words: *internal mobile phone antenna; penta-band operation; shorted planar monopole; spiral slot; GSM850/900/DCS/PCS/UMTS operation*

1. INTRODUCTION

Planar monopole antennas [1] are very promising for the application in the mobile phone as an internal antenna for their attractive advantages of broadband operation, low profile, compact size, and so on. A variety of internal multiband planar monopole antennas for mobile phone applications have also been reported in the open literature [1-10]. These antennas generally can cover GSM900 (880–960 MHz), DCS (1710–1880 MHz), PCS (1850–1990 MHz), and UMTS (1920–2170 MHz) bands. However, it is usually not an easy task for these designs to cover the desired GSM850 band (824–894 MHz) in their lower operating band at 900 MHz.

Recently, the resonant slot antenna has also been successfully applied for mobile phone application [11]. This type of slot antenna, however, is printed on the system circuit board of the mobile phone, thus occupying a certain valuable board space in the mobile phone. In this article, we demonstrate that the resonant slot antenna is also very promising to be embedded within the planar

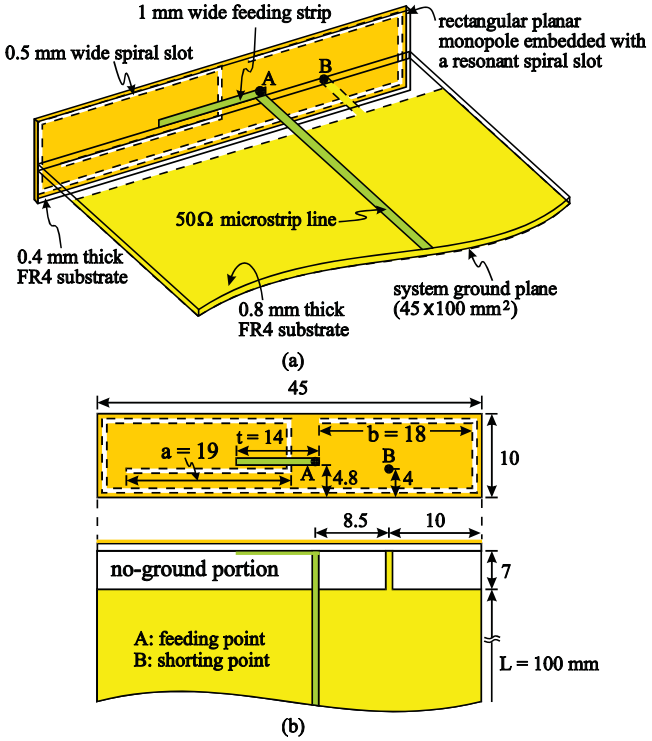

Figure 1 (a) Configuration of the internal shorted planar monopole antenna embedded with a resonant spiral slot for penta-band mobile phone operation. (b) Dimensions of the antenna. [Color figure can be viewed in the online issue, which is available at www.interscience.wiley.com]

monopole to form a new integrated antenna comprising the planar monopole and the resonant slot. In this case, the resonant slot does not occupy the valuable board space, and moreover, can generate additional resonant modes to greatly enhance the bandwidths of the lower and upper bands of the proposed integrated antenna as shown in Figure 1. With the proposed antenna, penta-band operation covering GSM850/900/DCS/PCS/UMTS bands can easily be achieved.

The proposed antenna is easy to fabricate by printing on an FR4 substrate of small size 10×45 mm^2, which is then placed above and perpendicular to the top edge, with a small distance of 7 mm, of the system ground plane. This arrangement leaves a top no-ground portion of the system circuit board between the planar monopole and the system ground plane. The no-ground portion can

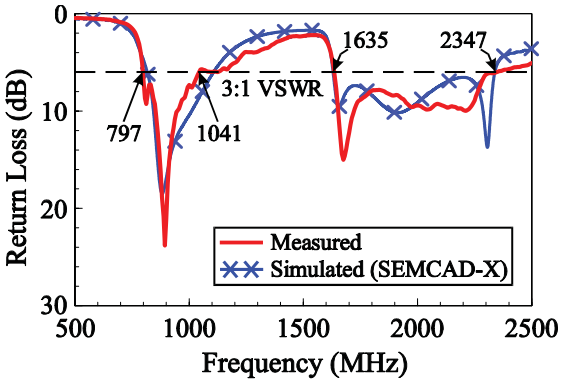

Figure 2 Measured and simulated return loss for the antenna shown in Figure 1. [Color figure can be viewed in the online issue, which is available at www.interscience.wiley.com]

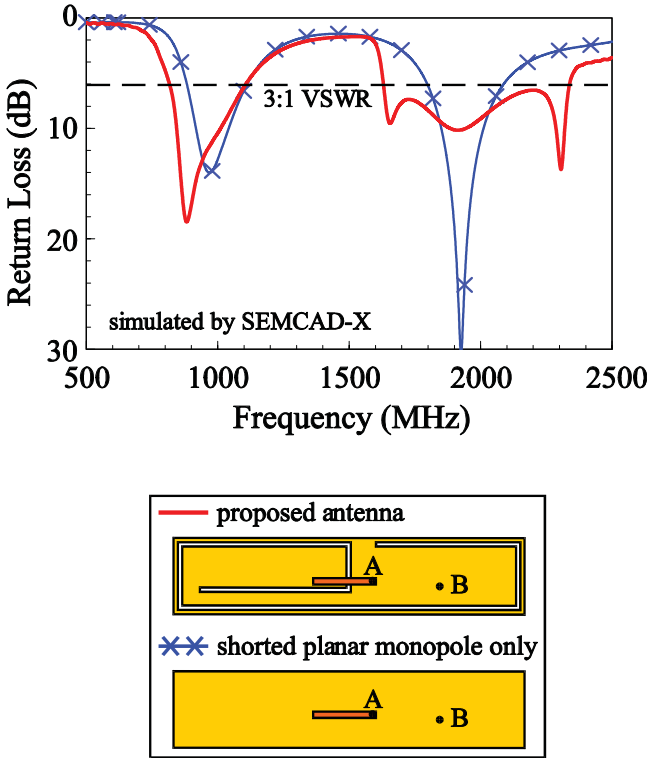

Figure 3 Simulated return loss for the proposed antenna and the case with the shorted planar monopole only (without the resonant spiral slot); corresponding dimensions are the same as given in Figure 1. [Color figure can be viewed in the online issue, which is available at www.interscience.wiley.com]

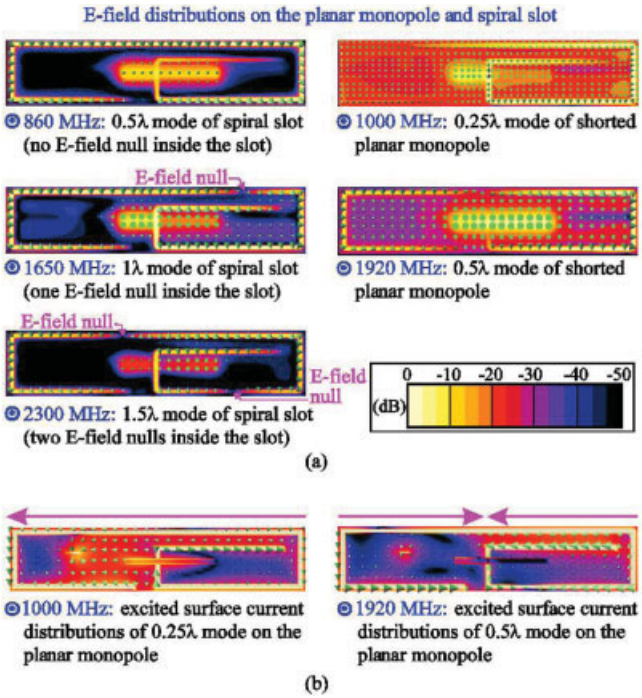

Figure 4 (a) Simulated E-field distributions on the shorted planar monopole and resonant spiral slot at 860, 1000, 1650, 1920, and 2300 MHz. (b) Simulated excited surface current distributions on the shorted planar monopole at 1000 and 1920 MHz. [Color figure can be viewed in the online issue, which is available at www.interscience.wiley.com]

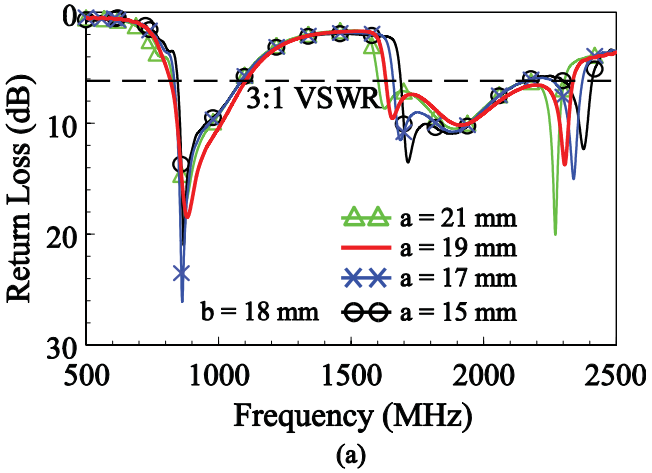

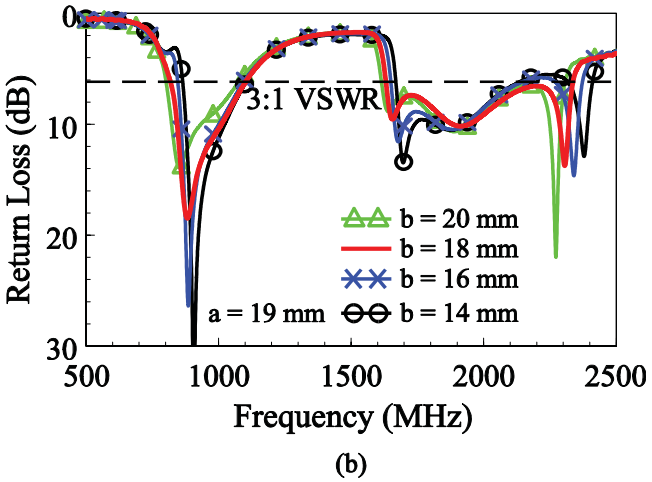

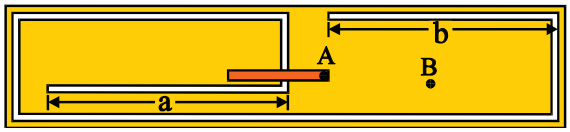

Figure 5 Simulated return loss for the proposed antenna (a) as a function of the feed-slot portion length *a*, and (b) as a function of the end-slot portion length *b*; other parameters are the same as given in Figure 1. [Color figure can be viewed in the online issue, which is available at www.interscience.wiley.com]

be reused to accommodate the associated electronic components, such as the speaker, to achieve a compact integration of the antenna inside the mobile phone. Detailed experimental and simulation results of the proposed antenna, including the case of integrating the speaker of the mobile phone, are presented and discussed. Effects of the user's hand [12-18] on the performances of the proposed antenna are also analyzed. In this study, SPEAG SEMCAD-X (Simulation platform for EMC, Antenna design, and Dosimetry) simulation software [19] is used for the simulation studies.

2. GEOMETRY OF THE PROPOSED ANTENNA

The configuration of the proposed antenna is shown in Figure 1(a), and detailed dimensions of the antenna are shown in Figure 1(b). The antenna mainly comprises a simple rectangular planar monopole of size 10×45 mm^2 and a 0.5-mm wide spiral slot of length

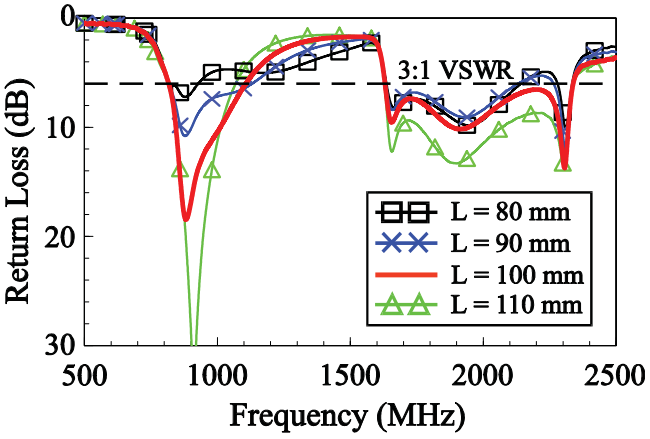

Figure 6 Simulated return loss for the proposed antenna as a function of the groundplane length *L*; other parameters are the same as given in Figure 1. [Color figure can be viewed in the online issue, which is available at www.interscience.wiley.com]

108 mm embedded therein. Both the planar monopole and the spiral slot are printed on a 0.4-mm thick FR4 substrate, which is placed perpendicular to the top edge of the system circuit board (0.8-mm thick FR4 substrate used here), with a small distance of 7 mm to the system ground plane of length 100 mm (*L*) and width 45 mm printed on the back side of the circuit board. The FR4

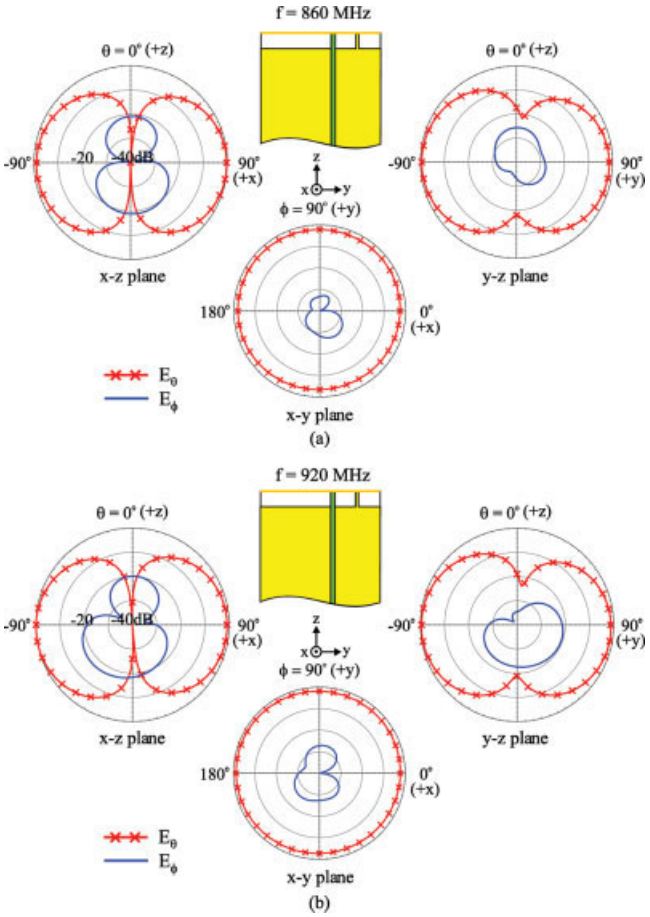

Figure 7 Measured radiation patterns for the proposed antenna. (a) 860 MHz (b) 920 MHz. [Color figure can be viewed in the online issue, which is available at www.interscience.wiley.com]

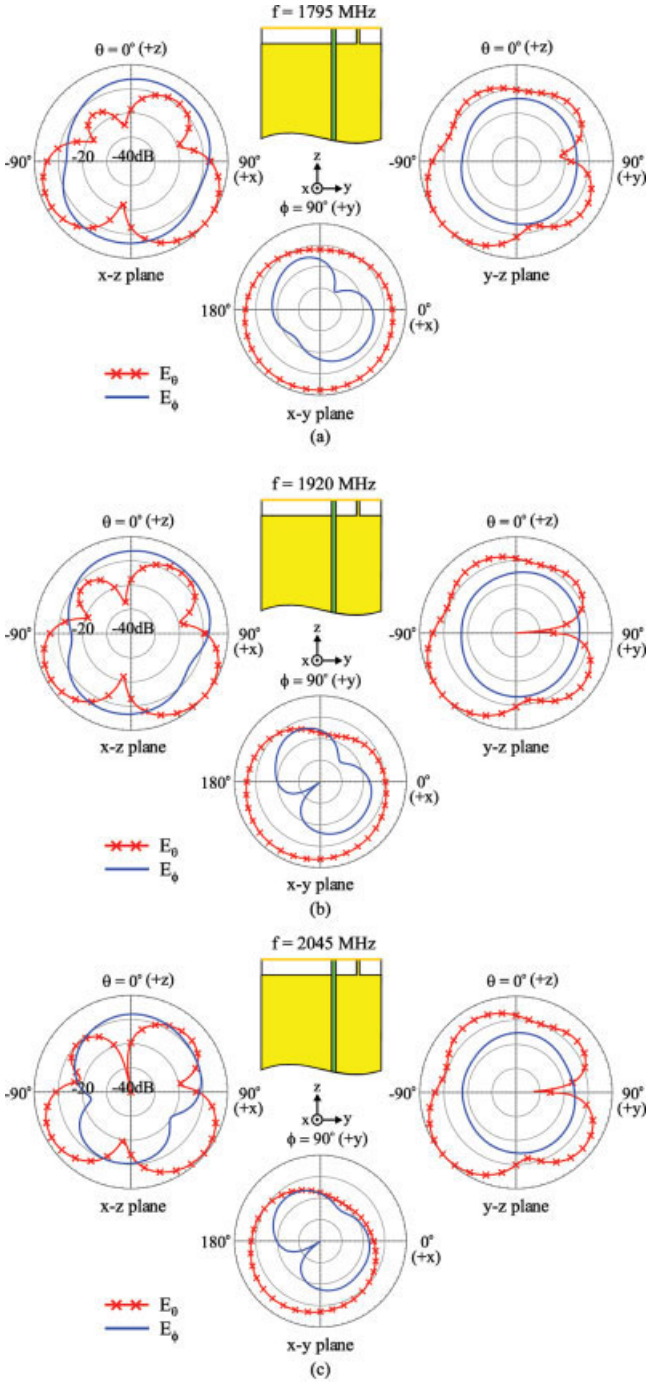

Figure 8 Measured radiation patterns for the proposed antenna. (a) 1795 MHz (b) 1920 MHz (c) 2045 MHz. [Color figure can be viewed in the online issue, which is available at www.interscience.wiley.com]

substrates used here have a relative permittivity of 4.4, and their conductivity is 0.0056 S/m at 920 MHz and 0.012 S/m at 1900 MHz. There is a no-ground portion of size 7 × 45 mm^2 between the planar monopole and the system ground plane, and a metal strip printed on the no-ground portion short-circuits the planar monopole at point B (the shorting point) to the system ground plane.

To excite both the planar monopole and the spiral slot, a 1-mm wide feeding strip of length 14 mm (*t*) printed on the other side of the antenna is used. The feeding strip is located about along the centerline of the planar monopole and also parallel to the top edge of the system circuit board, and its one end (point A, the feeding point) is connected to the 50-Ω microstrip feedline printed on the front side of the system circuit board. The feeding strip is also extended across the spiral slot and capacitively couples the energy from the microstrip feedline to the planar monopole and the spiral slot. To achieve good impedance matching of the proposed antenna, the distance between points A and B is determined to be 8.5 mm.

With the proposed design, the resonant modes of the rectangular planar monopole (quarter- and half-wavelength modes) and the spiral slot (half-, one-, and 1.5- wavelength modes) can be successfully excited to form two wide operating bands at about 900 and 1900 MHz to cover GSM850/900 and DCS/PCS/UMTS operation, respectively. Note that the length of the spiral slot is selected to be 108 mm and its three excited resonant modes in this design are at about 860, 1650, and 2300 MHz. The three additional resonant modes can be controlled by the feed-portion slot length *a* (19 mm here) and the end-portion slot length *b* (18 mm here) and can greatly enhance the bandwidths of the antenna's lower and upper bands. Details of the related results are analyzed with the aid of Figures 3–5 in the next section.

The no-ground portion between the planar monopole and the system ground plane can also be reused to accommodate the associated electronic components, such as the speaker discussed in this study. To test the integration of the speaker in the no-ground portion, a simulation model of the speaker is presented, and the

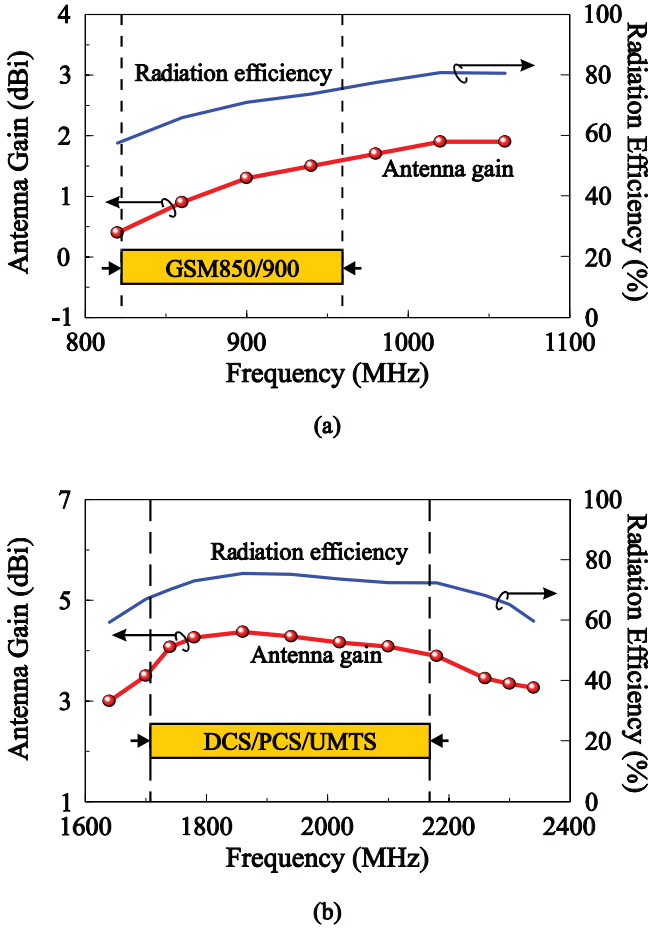

Figure 9 Measured antenna gain and simulated radiation efficiency for the proposed antenna (a) GSM850/900 band (b) DCS/PCS/UMTS band. [Color figure can be viewed in the online issue, which is available at www.interscience.wiley.com]

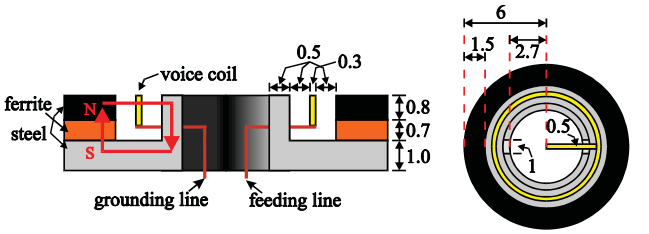

	ε_r	σ (S/m)
ferrite	12.5	0.01
steel	1.0	1.1 E6

material parameters

(a)

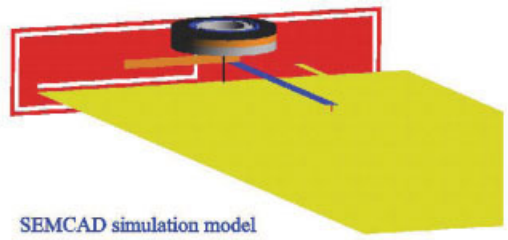

(b)

Figure 10 (a) Simulation model of the integrated speaker (b) Simulation model of the antenna with the integrated speaker. [Color figure can be viewed in the online issue, which is available at www.interscience.wiley.com]

simulated results are presented and discussed (see Figs. 10 and 11 in Section 3). Effects of the user's hand on the antenna performances are also studied in Figures 12–14. For the study on the effects of the integrated speaker and the user's hand, a plastic housing enclosing the antenna is added to secure the speaker (the speaker is attached to the inner surface of the housing) and also to avoid the user's hand directly contacting the antenna. The plastic housing has a relative permittivity of 3.5, and its conductivity is 0.01 S/m at 900 MHz and 0.02 S/m at 2000 MHz, respectively.

3. RESULTS AND DISCUSSION

Figure 2 shows the measured and simulated return loss for the proposed antenna with dimensions given in Figure 1. Agreement between the measurement and simulation is seen. Two wide operating bands centered at about 900 and 2000 GHz are excited with good impedance matching. The impedance bandwidths for the lower and upper bands, with a definition of 3:1 VSWR (6 dB return loss), are as large as 244 MHz (797–1041 MHz) and 712 MHz (1635–2347 MHz), respectively, and cover GSM850/900/DCS/PCS/UMTS penta-band operation.

Figure 3 shows a comparison of the simulated return loss for the proposed antenna and the case with the shorted planar monopole only (without the resonant spiral slot). The corresponding dimensions are the same as given in Figure 1. It is seen that the shorted planar monopole provides a fundamental (quarter-wavelength) mode at about 1000 MHz and a second (half-wavelength) mode at about 1920 MHz. With the presence of the spiral slot, the fundamental resonant mode of the shorted planar monopole is slightly decreased to be at about 960 MHz, and an additional half-wavelength mode of the spiral slot at about 820 MHz is generated. The two modes are formed into a wide lower band for the antenna to cover GSM850/900 operation. For the upper band, two additional resonant modes at about 1650 and 2300 MHz are generated, which are the 1- and 1.5-wavelength modes of the spiral slot. Similarly, the two additional modes and the half-wavelength mode of the planar monopole are formed into a wide upper band for the antenna to cover DCS/PCS/UMTS operation.

To explain in more detail the excited resonant modes of the proposed antenna, electric-field (E-field) distributions on the planar monopole and the spiral slot are presented in Figure 4(a). Strong E-field distributions inside the spiral slot at 860, 1650, and 2300 MHz are observed, which indicate that the half-, 1- and 1.5-wavelength resonant modes of the spiral slot antenna are excited. On the other hand, strong E-field distributions on the planar monopole at 1000 and 1920 MHz are also seen, which indicate that the quarter- and half-wavelength resonant modes of the planar monopole are excited. This can also be seen clearly from the simulated excited surface current distributions on the planar monopole at 1000 and 1920 MHz shown in Figure 4(b).

Effects of the feed-portion and end-portion slot lengths a and b are studied in Figures 5(a) and 5(b). From the results, some variations on the three excited resonant modes of the spiral slot are seen, while those of shorted planar monopole are very slightly affected. The results indicate that, by adjusting the slot lengths a and b, the slot's resonant modes can be controlled independently, with almost no effects on the resonant modes of the planar monopole. This behavior is similar to the fine-tuning of the slot lengths for adjusting the excited resonant modes of the slot antenna in [11].

Figure 6 shows the simulated return loss for the groundplane length L varied from 80 to 110 mm. Large effects on the impedance matching of the frequencies over the lower band are observed. For $L = 90$ mm, however, the obtained lower band can still cover GSM850/900 operation. For the upper band, when the length L is decreased to be 80 mm, the impedance matching can still be

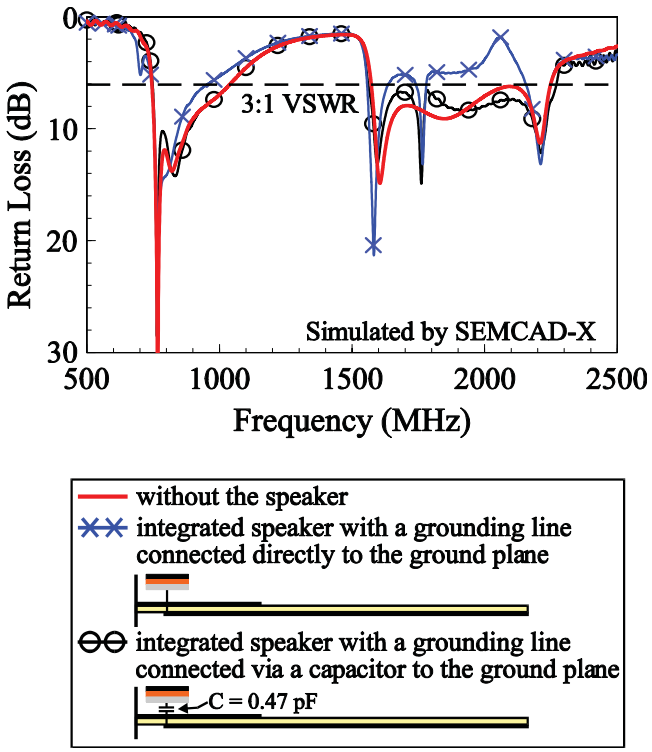

Figure 11 Simulated return loss for the proposed antenna without and with the integrated speaker; the latter includes the cases of the speaker connected directly or via a capacitor to the system ground plane. [Color figure can be viewed in the online issue, which is available at www.interscience.wiley.com]

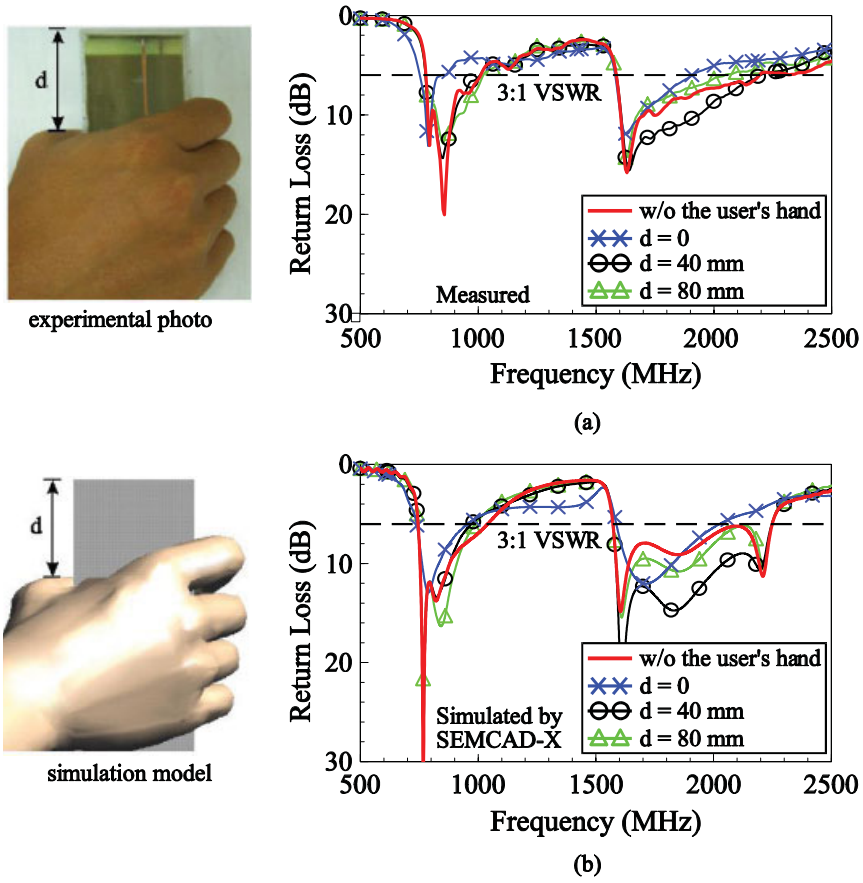

Figure 12 (a) Measured and (b) simulated return loss for $d = 0$, 40, and 80 mm for the proposed antenna enclosed by a 1-mm thick plastic housing and held by the user's hand; the case without the user's hand is also shown for comparison. [Color figure can be viewed in the online issue, which is available at www.interscience.wiley.com]

better than 3:1 VSWR, except for a small frequency range around 2250 MHz which is still better than about 5 dB return loss (3.5:1 VSWR). In this case, the obtained upper band can still cover DCS/PCS/UMTS operation for practical applications.

Figures 7(a) and 7(b) shows the measured radiation patterns at 860 and 920 MHz, the center frequencies of GSM850 and GSM900 bands. Monopole-like radiation patterns at the two frequencies are seen, which are similar to the radiation patterns of the conventional mobile phone antenna for GSM operation [1]. This is due to the fact that the radiation patterns are mainly dominated by the current distributions on the system ground plane for GSM operation, since the system ground plane of the mobile phone is an efficient radiator at about 900 MHz [20].

For the upper band, measured radiation patterns at 1795, 1920, and 2045 MHz, the center frequencies of DCS/PCS/UMTS bands, are plotted in Figures 8(a–c), respectively. The obtained patterns are also similar to those of the conventional mobile phone antennas [1] for the 1800-MHz band operation. Stable radiation patterns over the lower and upper bands are also observed, which is advantageous for practical applications. Figure 9 presents the measured antenna gain and simulated radiation efficiency over the lower and upper bands. For the lower band, the antenna gain is varied in a small range of 0.4–1.3 dBi, and the radiation efficiency is all better than 60%. For the upper band, the antenna gain is varied from 3.3 to 4.2 dBi, while the radiation efficiency is larger than 65%.

The integration of the speaker and the user's hand effects are also studied. The simulation model of the integrated speaker is given in Figure 10(a), and the total simulation model of the antenna with the integrated speaker is shown in Figure 10(b). In the study, the top side of the speaker is attached to the inner surface of the plastic housing. The bottom sides of the speaker are grounded to the system ground plane directly or via a small capacitor of 0.47 pF (see the insets in Fig. 11). The latter case with a small capacitor is used to suppress the excited surface currents on the system ground plane from entering the speaker; this can reduce the coupling effects of the speaker on the performances of the antenna. Figure 11 shows the simulated return loss for the proposed antenna without and with the integrated speaker; the latter includes the cases of the speaker connected directly or via a capacitor to the system ground plane. Results clearly indicate that the impedance matching over the upper band is degraded after the integration of the speaker connected directly to the system ground plane. However, when a small capacitor is added, the impedance matching over the upper band is effectively improved. Over the lower band, the resonant modes are very slightly affected with the integration of the speaker and still cover the desired GSM850/900 operating band.

Figure 12 shows measured and simulated return loss for the antenna held by the user's hand with $d = 0$, 40, and 80 mm, and the corresponding simulation model and experimental photo are also shown. The user's hand model includes a forearm, which is important in the simulation study, and the material parameters of the simulation model are provided by SPEAG SEMCAD [19]. The material parameters include muscle (925 MHz: $\varepsilon_r = 54.9$, $\sigma = 0.95$ S/m; 1795 MHz: $\varepsilon_r = 53.6$, $\sigma = 1.34$ S/m), skin (925 MHz:

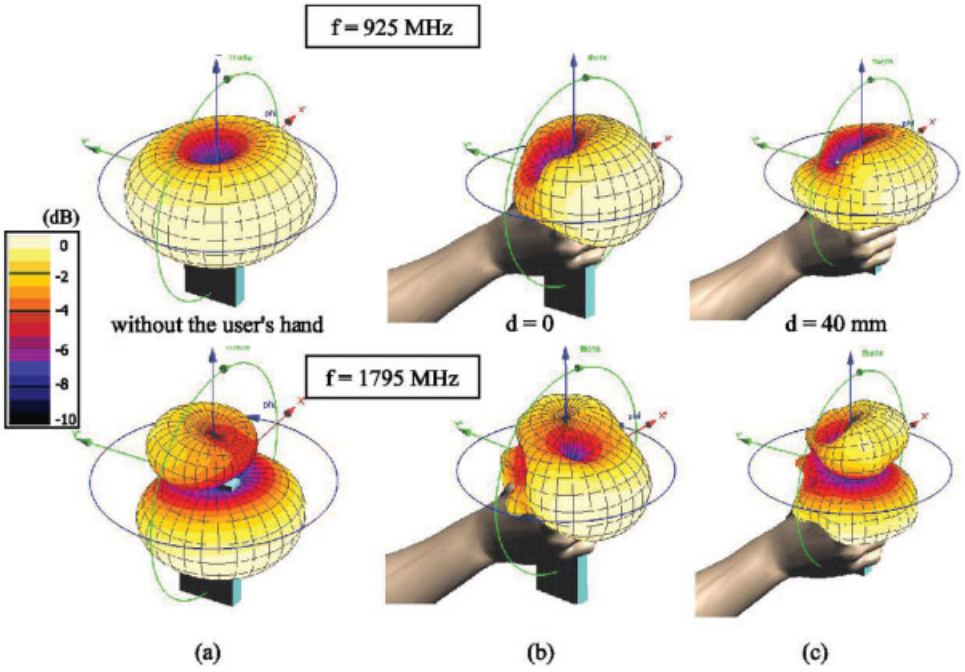

Figure 13 Simulated radiation patterns at 925 and 1795 MHz for the proposed antenna enclosed by a 1-mm thick plastic housing. (a) Without the user's hand. (b) With the user's hand, $d = 0$. (b) With the user's hand, $d = 40$ mm. [Color figure can be viewed in the online issue, which is available at www.interscience.wiley.com]

$\varepsilon_r = 41.3$, $\sigma = 0.87$ S/m; 1795 MHz: $\varepsilon_r = 38.9$, $\sigma = 1.18$ S/m), and bones (925 MHz: $\varepsilon_r = 20.7$, $\sigma = 0.34$ S/m; 1795 MHz: $\varepsilon_r = 19.3$, $\sigma = 0.59$ S/m). In the study, the parameter d is defined to be the distance from the top edge of the thumb portion to the top edge of the plastic housing. By comparing the simulated results in Figure 12(b) with the measured data in Figure 12(a), agreement between the measurement and simulation is ensured. Large effects of the user's hand on the impedance matching of the antenna are also seen, especially for the case of $d = 0$ (the antenna is totally enclosed by the user's hand). This behavior will also cause large effects in the antenna's radiation characteristics.

Figure 13 plots the simulated three-dimensional total radiation patterns at 925 and 1795 MHz for the cases without the user's hand and $d = 0$, 40 mm. For the patterns at 925 MHz, owing to the presence of the user's hand, the radiation patterns are no longer monopole-like as shown in Figure 7. It is also seen that the radiation power is greatly absorbed by the user's hand in the forearm direction for $d = 0$. For 1795 MHz, similar behavior is observed, and large distortions in the radiation patterns, especially in the user's forearm direction, are seen.

Figure 14 shows the simulated radiation efficiency as a function of d for the antenna. Large decrease in the radiation efficiency owing to the presence of the user's hand is seen, and the efficiency is decreased with a decrease in d. For the case of 925 MHz, the radiation efficiency is decreased from about 75% in free space to about 20% for $d = 0$. For the case of 1795 MHz, the radiation efficiency is decreased from about 70% in free space to about 30% for $d = 0$.

4. CONCLUSION

An internal shorted planar monopole antenna embedded with a resonant spiral slot for penta-band mobile phone application has been proposed and studied. Both of the planar monopole and the spiral slot can generate resonant modes to form two wide operating bands centered at about 900 and 2000 MHz for covering GSM850/900 and DCS/PCS/UMTS operation. The planar monopole and the spiral slot are easily fabricated on a thin FR4 substrate and occupy a small area of 10×45 mm^2. They can also be placed with a small distance of 7 mm above the top edge of the system circuit board, and is promising to operate as an internal antenna for the mobile phones. Good radiation characteristics of the antenna over the operating bands have also been observed. In addition, effects on the antenna performances for the proposed antenna integrated with a speaker and held by the user's hand have been studied and analyzed. Results show that the speaker effects on the antenna performances can be greatly suppressed or eliminated by adding a small capacitor between the speaker and the system ground plane. When the antenna is held by the user's hand, there are large decreases in the radiation efficiency of the antenna, and strong

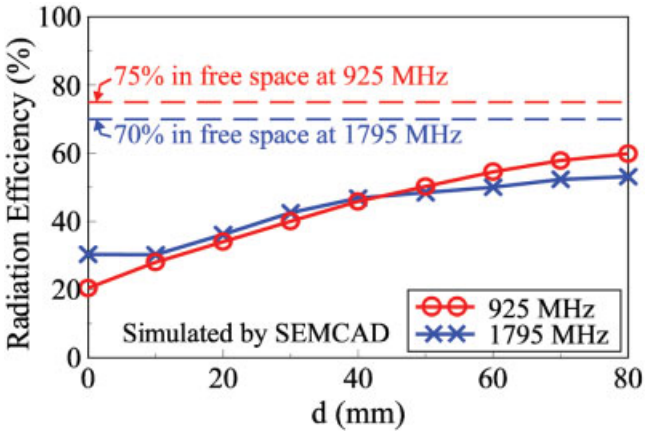

Figure 14 Simulated radiation efficiency as a function of d for the proposed antenna enclosed by a 1-mm thick plastic housing and held by the user's hand. [Color figure can be viewed in the online issue, which is available at www.interscience.wiley.com]

effects in the radiation patterns in the forearm direction are also observed as well, which are similar to the observations for the conventional internal mobile phone antennas [14-18].

ACKNOWLEDGMENTS

The generous support of Schmid & Partner Engineering AG (SPEAG) for SEMCAD-X simulation software is greatly appreciated.

REFERENCES

1. K.L. Wong, Planar antennas for wireless communications, Wiley, New York, USA, 2003.
2. Y.W. Chow, E.K. Ning Yung, K.F. Tsang, and H. T. Hui, An innovative monopole antenna for mobile-phone handsets, Microwave Opt Technol Lett 25 (2000), 119-121.
3. P.L. Teng and K.L. Wong, Planar monopole folded into a compact structure for very-low-profile multiband mobile-phone antenna, Microwave Opt Technol Lett 33 (2002), 22-25.
4. C.Y. Chiu, P.L. Teng and K.L. Wong, Shorted, folded planar monopole antenna for dual-band mobile phone, Electron Lett 39 (2003), 1301-1302.
5. K.L. Wong, G.Y. Lee, and T. W. Chiou, A low-profile planar monopole antenna for multiband operation of mobile handsets, IEEE Trans Antennas Propag 51 (2003), 121-125.
6. P.L. Teng, C.Y. Chiu, and K. L. Wong, Internal planar monopole antenna for GSM/DCS/PCS folder-type mobile phones, Microwave Opt Technol Lett 39 (2003), 106-108.
7. C.C. Lin, H.C. Tung, H.T. Chen, and K. L. Wong, A folded metal-plate monopole antenna for multiband operation of a PDA phone, Microwave Opt Technol Lett 39 (2003), 135-138.
8. S.Y. Lin, Multiband folded planar monopole antenna for mobile handsets, IEEE Trans Antennas Propag 52 (2004), 1790-1794.
9. T.K.W. Low, Z.N. Chen, and N. Yang, Bent planar monopole operating at GSM/ DCS/PCS/IMT2000 quad-bands, Microwave Opt Technol Lett 40 (2004), 170-172.
10. Y.S. Shin, S.O. Park, and M. Lee, A broadband interior antenna of planar monopole type in handsets, IEEE Antennas Wireless Propag 4 (2005), 9-12.
11. K.L. Wong, Y.W. Chi, and S. Y. Tu, Internal multiband printed folded slot antenna for mobile phone application, Microwave Opt Technol Lett 49 (2007), 1833-1837.
12. M. Francavilla, A. Schiavoni, P. Bertotto, and G. Richiardi, Effect of the hand on cellular phone radiation, IEE Proc Microwave Antennas Propag 148 (2001), 247-253.
13. O. Kivekas, J. Ollikainen, T. Lehtiniemi, and P. Vainikainen, Bandwidth, SAR, and efficiency of internal mobile phone antennas, IEEE Trans Antennas Propag 46 (2004), 71-86.
14. C.M. Su, C.H. Wu, K.L. Wong, S.H. Yeh, and C.L. Tang, User's hand effects on EMC internal GSM/DCS dual-band mobile phone antenna, Microwave Opt Technol Lett 48 (2006), 1563-1569.
15. C.H. Wu, K.L. Wong, C.I. Lin, C.M. Su, S.H. Yeh, and C.L. Tang, Simplified hand model including the user's forearm for the study of internal GSM/DCS mobile phone antenna, Microwave Opt Technol Lett 48 (2006), 2202-2205.
16. C.I. Lin, K.L. Wong, S.H. Yeh, and C.L. Tang, Study of an L-shaped EMC chip antenna for UMTS operation in a PDA phone with the user's hand, Microwave Opt Technol Lett 48 (2006), 1746-1749.
17. C.H. Wu and K.L. Wong, EMC internal GSM/DCS patch antenna for thin PDA phone application, Microwave Opt Technol Lett 49 (2007), 403-408.
18. C.I. Lin and K.L. Wong, Internal meandered loop antenna for GSM/DCS/PCS multiband operation in a mobile phone with the user's hand, Microwave Opt Technol Lett 49 (2007), 759-765.
19. http://www.semcad.com, SEMCAD, Schmid & Partner Engineering AG (SPEAG).
20. P. Vainikainen, J. Ollikainen, O. Kivekäs, and I. Kelander, Resonator-based analysis of the combination of mobile handsets antenna and chassis, IEEE Trans Antennas Propag 50 (2002), 1433-1444.

OPTIMIZATION OF POLYGONAL FRESNEL ZONE PLATES

Javier Alda[1] and Glenn Boreman[2]

[1] Applied Optics Complutense Group, University Complutense of Madrid, School of Optics, Av. Arcos de Jalón s/n., 28037 Madrid, Spain; Corresponding author: j.alda@opt.ucm.es

[2] CREOL, University of Central Florida, Orlando, FL 32816-2700

Received 16 July 2007

ABSTRACT: *The performance of Fresnel zone plates having polygonal boundaries between zones has been studied for polygons with a low number of sides. An optimized polygonal shape has been analytically defined by minimizing the mismatched area between the circular and the polygonal pseudo-Fresnel zones. The square polygon has been analyzed in more depth than the others because of its simple symmetry.* © 2007 Wiley Periodicals, Inc. Microwave Opt Technol Lett 50: 536–541, 2008; Published online in Wiley InterScience (www.interscience.wiley.com). DOI 10.1002/mop.23125

Key words: *Fresnel zone plates; diffractive optical elements; millimeter-wave*

1. INTRODUCTION

Fresnel zone plates (FZP) [1] are very useful additions in micro- and nano-photonic elements and devices [2]. They can be easily integrated as flat optical elements with focusing capabilities. The most common designs use circles to define the contours of the contiguous Fresnel zones. When the resolution of the fabrication techniques is comparable with the spatial dimensions of the Fresnel zones, the actual fabricated contours circles are jagged versions of the perfect circular pattern. For those cases, the study of polygons with a large number of sides has received attention [3, 4]. In this article, we are more interested in the analysis of FZP having polygonal contours with a low number of sides. Those cases may occur when the FZP needs to be fitted with elements or systems having a finite number of axes of symmetry: squares, hexagons, etc. In fact, square FZPs have been designed and tested in the past to compare their performance with the classical circular ones [2]. Some algorithms have been also developed to optimize the parameters of the square FZP [5]. In this article, we extend the analysis to the case of a regular polygon having an arbitrary number of sides, while emphasizing our interest and calculation for a polygon with a low number of sides. The performance of a given polygonal FZP is compared with a circular FZP having the same number of rings. As expected, we will see that this performance is better as the number of sides of the polygon increases.

Section 2 of the article presents the basis of the design procedure along with definitions of the important parameters and symmetries of the problem. Section 3 is devoted to the analysis of the results provided by a numerical simulation of the polygon elements within a scalar diffraction model, with special attention to the case of the square FZP. The conclusions of the article are described in Section 4.

2. GEOMETRICAL DESIGN

A FZP works by adding, blocking, or shifting in phase selected portions of the incoming wavefront that would otherwise interfere destructively. The increase in the irradiance obtained by the FZP is, to a first-order approximation, proportional to the square of the number of Fresnel zones included. However, losses caused by Fresnel reflection at the surface of the FZP surface, shadowing between adjacent zones, and departure from the initial design due